

## ORIGINAL ARTICLE

# Molecular effectors and modulators of hypericin-mediated cell death in bladder cancer cells

E Buytaert<sup>1</sup>, JY Matroule<sup>2</sup>, S Durinck<sup>3</sup>, P Close<sup>2</sup>, S Kocanova<sup>1</sup>, JR Vandenheede<sup>1</sup>, PA de Witte<sup>4</sup>, J Piette<sup>2</sup> and P Agostinis<sup>1</sup>

<sup>1</sup>Department Molecular and Cell Biology, Faculty of Medicine, Catholic University of Leuven, Brabant, Belgium; <sup>2</sup>Laboratory of Virology and Immunology, University of Liège, Liège, Belgium; <sup>3</sup>Department of Electrical Engineering, ESAT-SCD, Catholic University of Leuven, Brabant, Belgium and <sup>4</sup>Laboratory for Pharmaceutical Biology and Phytopharmacology, Faculty of Pharmacy, Catholic University of Leuven, Brabant, Belgium

**Photodynamic therapy (PDT) is an anticancer approach utilizing a light-absorbing molecule and visible light irradiation to generate, in the presence of O<sub>2</sub>, cytotoxic reactive oxygen species, which cause tumor ablation. Given that the photosensitizer hypericin is under consideration for PDT treatment of bladder cancer we used oligonucleotide microarrays in the T24 bladder cancer cell line to identify differentially expressed genes with therapeutic potential. This study reveals that the expression of several genes involved in various metabolic processes, stress-induced cell death, autophagy, proliferation, inflammation and carcinogenesis is strongly affected by PDT and pinpoints the coordinated induction of a cluster of genes involved in the unfolded protein response pathway after endoplasmic reticulum stress and in antioxidant response. Analysis of PDT-treated cells after p38<sup>MAPK</sup> inhibition or silencing unraveled that the induction of an important subset of differentially expressed genes regulating growth and invasion, as well as adaptive mechanisms against oxidative stress, is governed by this stress-activated kinase. Moreover, p38<sup>MAPK</sup> inhibition blocked autonomous regrowth and migration of cancer cells escaping PDT-induced cell death. This analysis identifies new molecular effectors of the cancer cell response to PDT opening attractive avenues to improve the therapeutic efficacy of hypericin-based PDT of bladder cancer.**

*Oncogene* (2008) 27, 1916–1929; doi:10.1038/sj.onc.1210825; published online 22 October 2007

**Keywords:** photodynamic therapy; microarrays; p38<sup>MAPK</sup>

## Introduction

Bladder cancer, the fourth most common malignancy in men and the ninth in women in the United States, is characterized by frequent recurrence and poor clinical outcome when tumors from noninvasive flat and papillary urothelial neoplasia progress to muscle invasive or metastatic disease (Sengupta *et al.*, 2004). Thus recognition of early-stage urothelial cancers and improvements in bladder cancer treatment are pressing needs. Photodynamic therapy (PDT) utilizes a tumor-localizing photosensitizer and visible light to produce reactive oxygen species (ROS) (Dolmans *et al.*, 2003). PDT efficacy relies on a combination of direct ROS-mediated cytotoxic effects, vascular damage and induction of inflammatory responses (Dolmans *et al.*, 2003; Castano *et al.*, 2006), indicating a critical role for the molecular interplay between cancer cells and the surrounding tumor environment in therapeutic outcome.

Hypericin is a powerful photocytotoxic sensitizer with pronounced tumor-localizing properties (Kamuhabwa *et al.*, 2004; Van De Putte *et al.*, 2005). We recently found that hypericin localizes in the neoplastic urothelium with higher specificity and selectivity to that displayed by aminolaevulinic acid, a precursor of the endogenous sensitizer protoporphyrin IX (D'Hallewin *et al.*, 2002). Thus, besides its exploitation for accurate fluorescent detection of these malignancies, hypericin may become the photosensitizer of choice for PDT of bladder cancer.

Previous studies showed that intracellularly, hypericin-PDT-induced cell death is mediated by endoplasmic reticulum (ER) Ca<sup>2+</sup> store emptying and executed through caspase-dependent or -independent pathways (Buytaert *et al.*, 2006). However, hypericin-PDT also activates rescuing responses, chiefly governed by the activation of p38<sup>MAPK</sup> (Assefa *et al.*, 1999; Hendrickx *et al.*, 2003). p38<sup>MAPK</sup>, of which four isoforms (p38- $\alpha$ , - $\beta$ , - $\gamma$  and - $\delta$ ) exist, is a member of the mitogen-activated protein kinase (MAPK) superfamily commonly activated by cellular stress, proinflammatory cytokines and growth factors (Zarubin and Han, 2005). Activated p38<sup>MAPK</sup> orchestrates various cellular responses including inflammation and survival but in certain contexts also cell death (Zarubin

Correspondence: Dr P Agostinis, Department Molecular and Cell Biology, KULeuven, Herestraat 49, Campus Gasthuisberg, Leuven, Brabant 3000, Belgium.

E-mail: patrizia.agostinis@med.kuleuven.be

Received 29 January 2007; revised 19 July 2007; accepted 5 September 2007; published online 22 October 2007

and Han, 2005). Recently, a tumor-promoting role for p38<sup>MAPK</sup> in prostate cancer (Park *et al.*, 2003), breast cancer (Tsai *et al.*, 2003; Suarez-Cuervo *et al.*, 2004), transformed follicular lymphoma (Elenitoba-Johnson *et al.*, 2003; Lin *et al.*, 2004) and leukemia (Liu *et al.*, 2000) has emerged. This suggests that inhibition of this signaling pathway may become therapeutically attractive, especially for hypericin-PDT, since the survival role of p38<sup>MAPK</sup> appears to be a distinguished molecular feature of this paradigm (Agostinis *et al.*, 2004).

Given the emerging clinical possibility of hypericin-PDT (hereafter called 'PDT') for bladder cancer, we found of crucial relevance to increase our still limited knowledge of the global tumor responses to PDT since the identification of molecular elements of cell death and survival pathways is required to develop new and improved therapeutic strategies.

In this study, we utilize oligonucleotide microarrays to examine the stress response of human bladder cancer cells to PDT at the genome-wide level and show that a central molecular feature of this paradigm is the coordinated induction of transcripts involved in the regulation of ER stress, cell death, antioxidant response, inflammation and carcinogenesis. Additionally, this study shows that inhibition of p38- $\alpha$  and - $\beta$  isoforms or p38<sup>MAPK</sup> silencing repress an important subset of PDT-induced genes involved in inflammation, growth and invasion as well as antioxidant defense mechanisms. Finally, we provide a proof-of-concept that activation of the p38<sup>MAPK</sup> signal transduction pathway increases tumorigenic potential of the surviving cancer cells after PDT.

## Results

### *Global distribution of hypericin-PDT differentially expressed genes*

To investigate molecular processes affected by PDT in T24 cells, we hybridized Affymetrix GeneChip HG-U133A 2.0 arrays with biotinylated cRNA from control and PDT-treated T24 cells. We analysed two independent experiments performed in duplicate, generating four hybridizations per condition. We evaluated a 7 h postirradiation time point, associated with 20–30% apoptotic cell death, to correlate microarray data with expression of key-induced genes at the protein level and evaluate biological effects of p38<sup>MAPK</sup> inhibition. Furthermore, two hybridizations from two independent experiments carried out 1 h postirradiation were also considered (data not shown), in order to single out early response genes (see Tables 1 and 2). Statistical filtering, retaining only genes with an increased or decreased expression of at least twofold and with an adjusted *P*-value <0.05, uncovered 826 genes significantly upregulated and 653 genes significantly downregulated by PDT, which were further annotated to Gene Ontology (GO) and subcategorized (Figure 1a). Of note, the class of metabolism and cell cycle/proliferation showed more genes repressed than upregulated, whereas the opposite was observed for genes involved in

transcription and signal transduction (Figure 1a) (see Supplementary data for complete lists of differentially expressed genes ordered by biological process). The top 10-induced genes visualized in the *M* versus *A* plot included the inducible cyclooxygenase (COX)-2 (*PTGS2*), molecular chaperones (*HSPA6*, *DNAJB9*), stress-responsive genes (*HMOX1*, activating transcription factor (*ATF*)3, *GDF15*), a Ras-related GTPase involved in dynamic organization of cytoskeleton proteins (*GEM*) and genes implicated in extracellular matrix (ECM) remodeling and invasion (*MMP1*, *MMP10*, *CSF2*). The top 10-repressed transcripts included genes with tumor-promoting roles (*ID3*, *SKP2*, *EDN1*, *ENC1*, *HOXA1*, *TGFB2*) and genes involved in inflammation (*CCL2*), apoptosis (*BCL2A1*), G-protein signaling (*RGS4*) and cell-cell adhesion (*PCDH7*) (Figure 1b).

### *Functional classification of hypericin-PDT-regulated genes and their p38<sup>MAPK</sup> dependence*

Functional characterization of differentially regulated genes by PDT allowed subcategorization of transcripts participating in carcinogenesis and signaling pathways relevant to therapy outcome. Additionally, investigation of the transcriptome of PDT-treated T24 cells in the presence of PD169316, a specific inhibitor of p38<sup>MAPK</sup>- $\alpha$  and - $\beta$ , unraveled downstream targets of this stress-activated protein kinase. These genes are grouped in Tables 1 or 2 when belonging to a cluster of p38<sup>MAPK</sup>-dependent genes.

*Cell death modulators.* An enriched class of upregulated genes consisted of heat shock protein (Hsps) family members (*HSPA6*, *DNAJB9*, *HSPH1*, *SERPINH1*, *HSPD1*, *HSPCB*), molecular chaperones known to regulate various adaptive intracellular responses allowing cell survival in stressful conditions (Calderwood *et al.*, 2006). Furthermore, a key feature of hypericin-PDT was the coordinated upregulation of proximal molecular sensors and effectors of the unfolded protein response (UPR) (Table 1), which is initiated by stress conditions perturbing ER homeostasis (Schroder and Kaufman, 2005). Correspondingly, the protein kinase *EIF2AK3* pancreatic ER kinase (PKR)-like ER kinase (PERK) and its downstream target eIF2 $\alpha$  (eukaryotic translation initiation factor 2 $\alpha$ ) were induced. Phospho-eIF2 $\alpha$  reduces protein load on the ER by stalling protein translation, while it paradoxically activates translation of certain mRNAs including that encoding for the transcription factor *ATF4*. Additionally, the *ATF4* transcriptional targets *DDIT3* (C/EBP homologous protein (CHOP)/GADD153) and *PPP1R15A* (Gadd34), which plays a role in translational recovery (Schroder and Kaufman, 2005), were upregulated while *CCND1*, a known PERK target leading to G<sub>1</sub> cell cycle arrest, was concurrently downregulated. The differential expression of several transcripts with an established role in the PERK-eIF2 $\alpha$ -ATF4 branch of the UPR required for CHOP expression is indicative of the validity of our microarray approach.

**Table 1** Selection of hypericin-PDT-induced differentially expressed genes

Probeset ID	Gene name	Description	FC ( $\log_2$ ratio)	P-value	
<i>Response to stimulus</i>					
<i>Response to unfolded protein</i>					
213418_at	<b>HSPA6</b>	Heat shock 70 kDa protein 6	11.64	1.01e-09	
202843_at	<i>DNAJB9</i>	DnaJ (Hsp40) homolog subfamily B member 9	5.91	4.87e-06	
208744_x_at	<i>HSPH1</i>	Heat shock 110 kDa protein	3.35	2.50e-05	
207714_s_at	<i>SERPINH1</i>	Collagen-binding protein 2 precursor (Hsp47)	2.1	0.000162	
200806_s_at	<i>HSPD1</i>	Heat shock 60 kDa protein	1.17	4.00e-05	
214359_s_at	<i>HSPCB</i>	Heat shock 90 kDa protein 1, $\beta$	1.11	5.60e-07	
<i>Response to ER stress</i>					
209383_at	<b>DDIT3</b>	DNA-damage inducible transcript 3 CHOP/GADD153	5.18	2.18e-05	UPR
202014_at	<b>PPP1R15A</b>	Protein phosphatase 1, regulatory subunit 15A, Gadd34	4.65	1.57e-07	UPR
217168_s_at	<i>HERPUD1</i>	Homocysteine-responsive ER-resident ubiquitin-like domain member 1 protein	2.8	4.42e-05	UPR
218696_at	<i>EIF2AK3</i>	Eukaryotic translation initiation factor 2 $\alpha$ kinase 3 precursor, PERK	1.57	0.000199	UPR
200970_s_at	<i>SERP1</i>	Stress-associated ER protein 1	1.13	0.000363	UPR
<i>Immune response</i>					
216598_s_at	<i>CCL2</i>	Small inducible cytokine A2 precursor	-3.37	0.001086	
<i>Metabolism</i>					
<i>Transcription factors</i>					
202672_s_at	<b>ATF3</b>	Cyclic AMP-dependent transcription factor ATF-3	9.18	2.35e-07	UPR
209189_at	<b>FOS</b>	Proto-oncogene protein c-fos	4.26	0.031901	
200779_at	<i>ATF4</i>	Activating transcription factor 4	2.18	6.50e-05	UPR
200670_at	<i>XBPI1</i>	X box-binding protein 1	1.86	0.000306	UPR
203752_s_at	<b>JUND</b>	Transcription factor jun-D	1.85	5.54e-05	
207826_s_at	<i>ID3</i>	DNA-binding protein inhibitor ID-3	-3.72	1.56e-05	
214639_s_at	<i>HOXA1</i>	Homeobox protein Hox-A1	-3.32	4.56e-07	
<i>ECM remodeling</i>					
204475_at	<i>MMP1</i>	Matrix metalloproteinase-1 precursor	7.16	1.89e-06	
205680_at	<i>MMP10</i>	Matrix metalloproteinase-10 precursor	5.99	1.40e-08	
<i>Signal transduction</i>					
204472_at	<b>GEM</b>	GTP-binding protein GEM (RAS-like protein KIR)	7.37	1.15e-06	
204339_s_at	<i>RGS4</i>	Regulator of G-protein signaling 4	-4.09	0.000386	
<i>Transport</i>					
212361_s_at	<i>ATP2A2</i>	Sarco/endoplasmic reticulum calcium ATPase 2 (SERCA2)	-1.78	0.000358	
<i>Cell cycle/proliferation</i>					
203626_s_at	<i>SKP2</i>	S-phase kinase-associated protein 2	-3.71	0.000349	
208711_s_at	<i>CCND1</i>	G <sub>1</sub> /S-specific cyclin-D1	-1.71	5.54e-05	UPR
<i>Cell communication/cell-cell signaling</i>					
221577_x_at	<i>GDF15</i>	Growth/differentiation factor 15 precursor	6.79	0.000270	
218995_s_at	<i>EDN1</i>	Endothelin-1 precursor	-3.81	0.002352	
<i>Autophagy</i>					
213836_s_at	<i>WIPI1</i>	WD-repeat domain phosphoinositide-interacting protein 1 (Atg18 protein homolog)	3.21	0.000466	
208786_s_at	<i>MAP1LC3B</i>	Microtubule-associated proteins 1A/1B light chain 3B precursor (Autophagy-related protein LC3 B)	1.8	2.99e-06	
213026_at	<i>ATG12</i>	Autophagy protein 12 (APG12-like)	0.99 <sup>s</sup>	1.79e-05	
<i>Apoptosis</i>					
206536_s_at	<i>BIRC4</i>	Baculoviral IAP repeat-containing protein 4, X-linked IAP	3.22	3.84e-06	
205214_at	<i>STK17B</i>	DAP kinase-related apoptosis-inducing protein kinase 2	3	1.83e-05	
218145_at	<i>TRIB3</i>	tribbles homolog 3, p65-interacting inhibitor of NF-kappaB	2.53	0.000560	UPR
201502_s_at	<i>NFKBIA</i>	NF- $\kappa$ B inhibitor $\alpha$	2.15	9.09e-07	
205681_at	<i>BCL2A1</i>	Bcl-2-related protein A1	-3.31	0.000174	
203685_at	<i>BCL2</i>	Apoptosis regulator Bcl-2	-2.26	0.000124	
202094_at	<i>BIRC5</i>	Baculoviral IAP repeat-containing protein 5, survivin	-1.37	4.46e-05	
<i>Development/differentiation/growth</i>					
201341_at	<i>ENC1</i>	Ectoderm-neural cortex 1 protein	-3.49	5.81e-06	
220407_s_at	<i>TGFB2</i>	Transforming growth factor $\beta$ -2 precursor	-3.35	0.000222	

**Table 1** (continued)

Probeset ID	Gene name	Description	FC ( $\log_2$ ratio)	P-value
<i>Cell adhesion</i>				
207029_at	<i>KITLG</i>	Kit ligand precursor (mast cell growth factor)	4.51	0.000100
205032_at	<i>ITGA2</i>	Integrin $\alpha$ -2 precursor (collagen receptor)	1.2	0.029848
205534_at	<i>PCDH7</i>	Protocadherin 7 precursor	-2.95	0.000395
201108_s_at	<i>THBS1</i>	Thrombospondin-1 precursor	-2.49	0.002129
204627_s_at	<i>ITGB3</i>	Integrin $\beta$ -3 precursor	-1.78	0.015801
204949_at	<i>ICAM3</i>	Intercellular adhesion molecule 3 precursor	-1.42	0.001297
202637_s_at	<i>ICAM1</i>	Intercellular adhesion molecule 1 precursor	-1.18	0.008778

Abbreviations: ER, endoplasmic reticulum; CHOP, C/EBP homologous protein; PERK, pancreatic ER kinase (PKR)-like ER kinase; UPR, unfolded protein response; ATF, activating transcription factor; ECM, extracellular matrix; SERCA, sarco(endoplasmic)-reticulum  $\text{Ca}^{2+}$ -ATPase; DAP, death-associated protein; NF- $\kappa$ B, nuclear factor- $\kappa$ B. Selected significantly ( $P < 0.05$ ) up- and downregulated genes in PDT-treated versus control T24 cells are presented according to biological process and ranked by fold change (FC) (as  $\log_2$  ratio). Genes detected upregulated 1 h after irradiation are marked in bold. Only genes with a  $\log_2$  ratio  $> |1|$  were included in the analysis, therefore genes presented with an induction below the threshold are indicated with '\$'. Transcripts involved in 'UPR' are indicated as such.

UPR activation was further evidenced by the concurrent upregulation of *XBPI* (X-box-binding protein 1), a transcription factor regulating various UPR-target genes including ER-resident chaperones (Schroder and Kaufman, 2005). Interestingly, *ATF3*, a highly PDT-induced stress gene (Figure 1b, Table 1) encoding a member of the ATF/cAMP-responsive element binding protein family of transcription factors, has been reported to be a PERK target (Jiang et al., 2004), suggesting a link between ATF3 induction and ER stress in our paradigm. PDT also upregulated *TRIB3*, a downstream negative modulator of the CHOP/ATF4 pathway (Ohoka et al., 2005), the ER protein *HERPUD1* which is involved in ER-associated degradation (ERAD), and *SERP1*, an ER translocon complex protein (Ma and Hendershot, 2004; Hori et al., 2006).

Moreover, PDT affected the expression of several genes controlling the apoptotic process (Table 1). Except for the induction of the inhibitor of apoptosis protein *BIRC4* (XIAP), PDT mostly repressed the expression of many antiapoptotic genes including *BCL2A1*, *BCL2* and *BIRC5* (survivin). Also, death-associated protein kinase-related apoptosis-inducing kinase 2 (*STK17B*) and  $\text{I}\kappa\text{B}\alpha$  (*NFKBIA*) were significantly induced by PDT.

Remarkably, crucial genes involved in autophagy induction, including *WIPI1* (human ortholog of the yeast autophagy-related gene (Atg18)), *MAP1LC3B* (human ortholog of the yeast Atg8) and *ATG12* (Table 1), were upregulated, thus suggesting that PDT increases the magnitude of the autophagic process.

*Cell-cell interaction and ECM remodeling.* Several transcripts regulating cell-cell and cell-matrix adhesion (*PCDH7*, *THBS1*, *ITGB3*, *ICAM3*, *ICAM1*), cell migration and cell-surface-mediated signal transduction (*KITLG*, *ITGA2*) and ECM remodeling (*MMP1*, *MMP10*, *MMP13*) were upregulated (Table 1). After PDT, surviving T24 cells lost their ability to attach and grow on plastic plates (data not shown), and only attached and proliferated in collagen type I-coated plates. This indicates that photosensitization alters the cells' adhesive property and creates permissive conditions for

cell attachment and persistence in collagen type I, a major component of the basal layer.

*p38<sup>MAPK</sup>-dependent targets.* Pretreating T24 cells with PD169316 prior to irradiation led to the significant repression of 27 and induction of two genes when compared to PDT-treated cells in the absence of the inhibitor (Table 2, see also 'Materials and methods' section).

p38<sup>MAPK</sup> inhibition affected the PDT-induced expression of immune and inflammatory response mediators, such as COX-2 (*PTGS2*), GM-CSF (granulocyte macrophage colony-stimulating factor; *CSF2*), interleukin 8 (*IL8*) and the Toll-like receptor 2, as also reported in previous studies (Hashimoto et al., 2000; Hoffmann et al., 2002; Imasato et al., 2002). Notably, the expression of a number of stress-responsive genes encoding antioxidant and Phase II drug-metabolizing enzymes (Table 2), with an established role in cellular protection following oxidative damage caused by ROS or electrophiles (Lee and Johnson, 2004) was found to be significantly attenuated by PD169316. This gene class, including *HMOX1*, *AKRIC1*, *AKRIC3*, *GCLC*, *GCLM*, *NQO1*, *TXNRD1*, *FTH1* and *MTIX* (Table 2), is regulated by binding of transcription factor Nrf2 (NF-E2-related factor 2) to the antioxidant response element, a cis-acting regulatory element found in their promoter regions (Lee et al., 2003; Lou et al., 2006). Particularly, PD169316 suppressed coordinately, albeit to a different extent, the induction of *AKRIC1*, *AKRIC3*, *GCLC* and *NQO1*, suggesting that p38<sup>MAPK</sup> activation stimulates Nrf2-dependent transcription following PDT. Moreover, p38<sup>MAPK</sup> inhibition caused partial downregulation of superoxide dismutase *SOD2* (Mn-SOD) induction, whose transcriptional activation through the Nrf2 pathway has not been reported so far.

Additional p38<sup>MAPK</sup>-dependent transcripts included genes involved in transcriptional regulation (*KLF11*, *PLAGL2*, *SIM2*, *CEBPD*), metabolic pathways (*ABCA1*, *INSR*, *DDAH2*), chromatin remodeling (*HIST1H2BG*, *HIST2H2AA*), cell death (*TNFRSF11B*, *STK3*), cell-cell signaling (*PTH1LH*, *EREG*), signal

**Table 2** Selection of hypericin-PDT-induced upregulated and p38<sup>MAPK</sup>-dependent genes

Probeset ID	Gene name	Description	FC log <sub>2</sub> ratio	P-value	+ PD16 (%)	
<i>Metabolism</i>						
<i>Arachidonic acid and prostaglandin metabolism</i>						
204748_at	<b>PTGS2</b>	Cyclooxygenase-2	8.68	1.32e-07	81.4	↓
210145_at	<i>PLA2G4A</i>	Cytosolic phospholipase A2	3.19	0.000708		
205128_x_at	<i>PTGS1</i>	Cyclooxygenase-1	2.33	0.000651		
203913_s_at	<i>HPGD</i>	15-Hydroxyprostaglandin dehydrogenase	1.78	0.033230		
<i>ECM remodeling</i>						
205959_at	<i>MMP13</i>	Matrix metalloproteinase-13 precursor	2.72	0.002174	100	↓
<i>Antioxidant and Phase II detoxifying enzymes</i>						
203665_at	<b>HMOX1</b>	Heme oxygenase-1	6.79	8.99e-09		
216594_x_at	<i>AKR1C1</i>	Aldo-keto reductase family 1 member C1	4.04	8.66e-06	91.9	↓
209160_at	<i>AKR1C3</i>	Aldo-keto reductase family 1 member C3	1.92	0.000769	100	↓
202922_at	<i>GCLC</i>	Glutamate-cysteine ligase catalytic subunit	2.2	7.19e-07	54	↓
215223_s_at	<i>SOD2</i>	Superoxide dismutase (Mn)	1.63	4.49e-06	43 <sup>s</sup>	↓
214211_at	<i>FTH1</i>	Ferritin heavy chain	1.5	4.31e-05		
203925_at	<i>GCLM</i>	Glutamate-cysteine ligase regulatory subunit	1.38	6.99e-07		
201266_at	<i>TXNRD1</i>	Thioredoxin reductase 1, cytoplasmic precursor	1.35	3.30e-06		
204326_x_at	<i>MT1X</i>	Metallothionein-1X	1.26	3.30e-05		
210519_s_at	<i>NQO1</i>	NAD(P)H dehydrogenase quinone 1	0.68 <sup>s</sup>	4.12e-05	31.2	↓
<i>Transcription factors</i>						
218486_at	<i>KLF11</i>	TGFβ-inducible early growth response protein 2	4.02	3.76e-08	13	↑
202924_s_at	<i>PLAGL2</i>	Zinc finger protein PLAGL2	1.96	0.000252	70.1	↓
201146_at	<i>NFE2L2</i>	Nuclear factor erythroid 2-related factor 2 (Nrf2)	1.27	5.83e-05		
206558_at	<i>SIM2</i>	Single-minded homolog 2	1.26	0.000800	57.1	↓
203973_s_at	<b>CEBPD</b>	CCAAT/enhancer-binding protein δ	1.13	5.80e-05	51.4	↓
<i>Metabolism (others)</i>						
203504_s_at	<i>ABCA1</i>	ATP-binding cassette subfamily A member 1	3.27	1.14e-07	85.2	↓
213792_s_at	<i>INSR</i>	Insulin receptor precursor	1.58	1.80e-07	53.3	↓
202262_x_at	<i>DDAH2</i>	Dimethylargininase 2	1.4	0.000466	53.7	↓
<i>Immune response</i>						
210229_s_at	<i>CSF2</i>	Granulocyte-macrophage colony-stimulating factor	7.03	4.47e-08	80.7	↓
213112_s_at	<b>SQSTM1</b>	Sequestosome-1 (ubiquitin-binding protein p62)	5.05	1.24e-07	67.2	↓
211506_s_at	<b>IL8</b>	Interleukin-8 precursor	1.65	0.000641	60.8	↓
204924_at	<i>TLR2</i>	Toll-like receptor 2 precursor	1.63	0.000882	95.9	↑
<i>Signal transduction</i>						
209568_s_at	<i>RGL1</i>	Ral guanine nucleotide dissociation stimulator-like 1	2.4	0.003212	100	↓
219500_at	<i>CLCF1</i>	B-cell-stimulating factor 3 precursor	1.34	0.002975	100	↓
<i>Development/differentiation/growth</i>						
205923_at	<i>RELN</i>	Reelin precursor	3.02	7.77e-06	76.8	↓
211527_x_at	<i>VEGF</i>	Vascular endothelial growth factor A precursor	2.86	0.000844		
<i>Cell organization and biogenesis</i>						
208490_x_at	<b>HIST1H2BG</b>	Histone H2B.a/g/h/k/l	1.65	0.000102	61	↓
218280_x_at	<b>HIST2H2AA</b>	Histone H2A type 2	1.14	0.011047	100	↓
<i>Cell death</i>						
204933_s_at	<i>TNFRSF11B</i>	TNF receptor superfamily member 11B precursor	4.1	9.62e-05	93.2	↓
211078_s_at	<i>STK3</i>	Serine/threonine-protein kinase 3	1.09	0.000552	45.7	↓
<i>Cell communication/cell-cell signaling</i>						
206300_s_at	<i>PTH1LH</i>	Parathyroid hormone-related protein precursor	2.1	0.001191	100	↓
205767_at	<b>EREG</b>	Epiregulin precursor	2.07	4.30e-06	46	↓
<i>Cell adhesion</i>						
210689_at	<i>CLDN14</i>	Claudin 14	5.5	8.42e-09	56.2	↓
<i>Others</i>						
210143_at	<i>ANXA10</i>	Annexin A10 (annexin 14)	3.81	7.77e-06	70.9	↓
213797_at	<i>RSAD2</i>	Radical S-adenosyl methionine domain containing 2	2.33	1.47e-08	76	↓
209277_at	<i>TFPI2</i>	Tissue factor pathway inhibitor 2 precursor	1.04	0.000431	100	↓

Abbreviations: ECM, ; extracellular matrix; TNF, tumor necrosis factor. Selected significantly ( $P < 0.05$ ) upregulated genes in PDT-treated versus control T24 cells are presented according to biological process and ranked by fold change (FC) (as log<sub>2</sub> ratio). p38<sup>MAPK</sup> dependence (up- or downregulation by 1 μM PD169316 as shown by the arrows) is indicated as percentage (%) of differential gene expression of PDT-treated versus control T24 cells. Genes detected upregulated 1 h after irradiation are marked in bold. Only genes with a log<sub>2</sub> ratio  $> |1|$  were included in the analysis, therefore genes presented with an induction or decrease below the threshold are indicated with 's'.

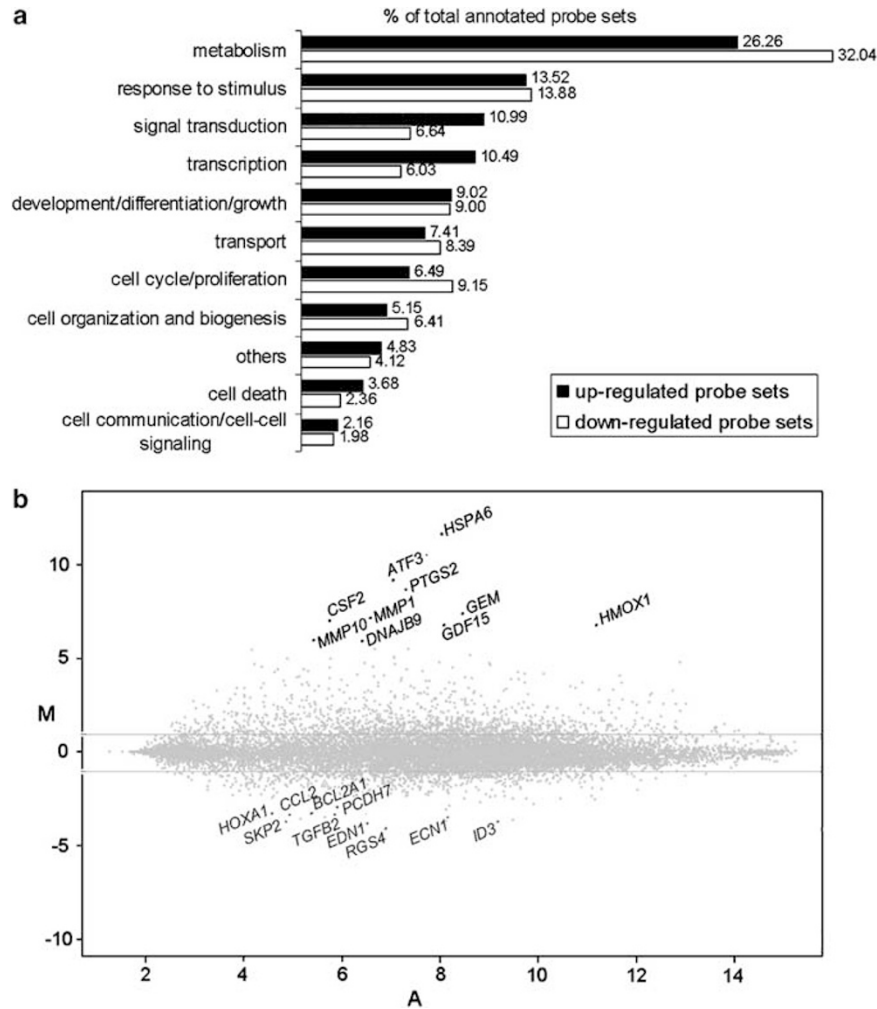


**Figure 1** (a) Functional overview of PDT-induced differentially expressed genes. Significantly ( $P < 0.05$ ) up- and downregulated probe sets in PDT-treated T24 cells were annotated to Gene Ontology (GO) terms in the category of biological process as described in 'Materials and methods' section. 'Others' are GO terms not included in categories listed above. Note that probe sets can be annotated to more than one GO term. (b) M versus A plot representing PDT-induced differentially expressed genes. Significantly ( $P < 0.05$ ) up- and downregulated probe sets in PDT-treated T24 cells on an  $M$  ( $\log_2$  ratio) versus  $A$  (average intensity) plot. Nondifferentially expressed genes are on the  $M = 0$  line.  $M = 1$  and  $M = -1$  lines indicate the applied threshold of fold increase of 2 and decrease of  $-2$ . The 10 most up- and downregulated genes, indicated by their gene name, are described in Tables 1 or 2, as specified in the text.

transduction (*RGL1*, *CLCF1*), development/differentiation/growth (*RELN*) and cell adhesion (*CLDN14*). Of note,  $p38^{\text{MAPK}}$  was required for the PDT-mediated upregulation of the ECM remodeling gene *MMP13*. The expression of relevant cell death modulators, including CHOP and Gadd34, as well as some  $p38^{\text{MAPK}}$ -regulated genes, such as COX-2 and IL-8, was affected early after PDT (for example, 1 h), suggesting that these targets contribute to the early cellular responses induced by PDT.

#### Validation of the microarray results by real-time quantitative PCR and western blotting

To verify PDT-mediated changes in transcript levels detected by microarray analysis, we performed qRT-PCR for a selection of relevant differentially expressed genes, which were strongly upregulated by PDT (*MMP1*, *MMP10*, *HMOX1*) and significantly inhibited by PD169316 (*MMP13*, *AKR1C1*). Fold changes from

qRT-PCR of all genes analysed in T24 cells correlated well with microarray analysis results (Figure 2a). Moreover, in conformity with the microarray data (Table 2), *MMP13* and *AKR1C1* upregulation after PDT in T24 cells was virtually abolished in the presence of PD169316. Although not evidenced by the microarray analysis (Table 2), PD169316 attenuated *HMOX1* induction by PDT (Figure 2a). To validate the general relevance of the results obtained with T24 cells, qRT-PCR of the selected genes was also performed in the low-grade, papillary bladder cancer cell line RT4. In PDT-treated RT4 cells, mRNA induction of *MMP1* and *MMP10* correlated well with the qRT-PCR results of T24 cells (Figure 2a), although in general mRNA induction in RT4 cells was somehow lower at 7 h after PDT. The induction of *MMP13*, *HMOX1* and *AKR1C1* in RT4 cells was also strongly  $p38^{\text{MAPK}}$  dependent (Figure 2b), thus extending the significance of the identified molecular targets to

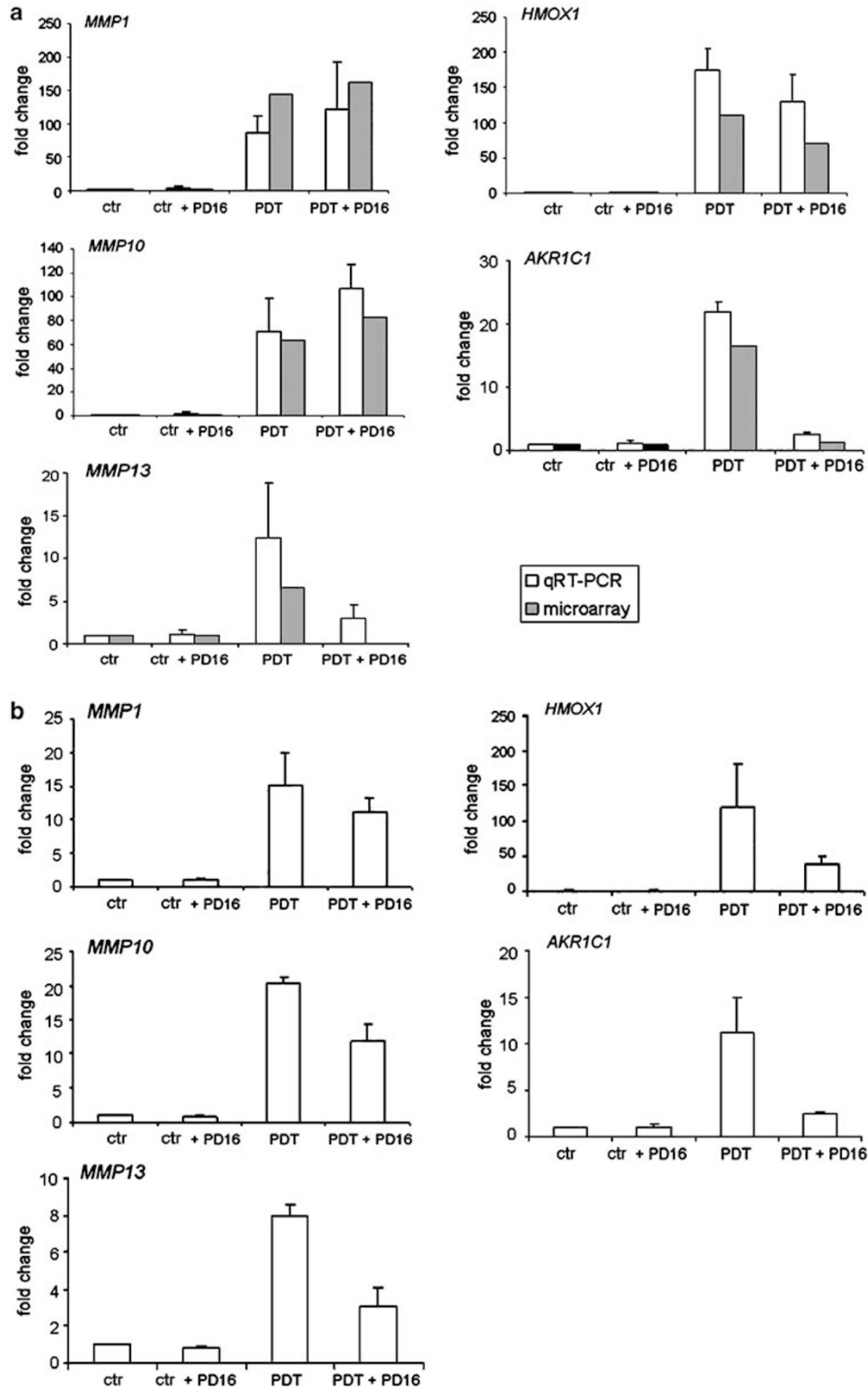


**Figure 2** Validation of microarray data by qRT-PCR. Total RNA was extracted from photodynamic therapy (PDT)-treated and control T24 (a) and RT4 (b) cells in the absence or presence of 1  $\mu$ M PD169316, at 7 h after irradiation. mRNA levels, expressed as fold change, of *MMP1*, *MMP10*, *MMP13*, *AKR1C1* and *HO-1* were analysed by qRT-PCR (a and b) and microarray analysis (a). Error bars represent s.d. of at least three qRT-PCR reactions performed on RNA from two independent experiments (for *AKR1C1* and results from RT4 cells, RNA from one experiment was used).

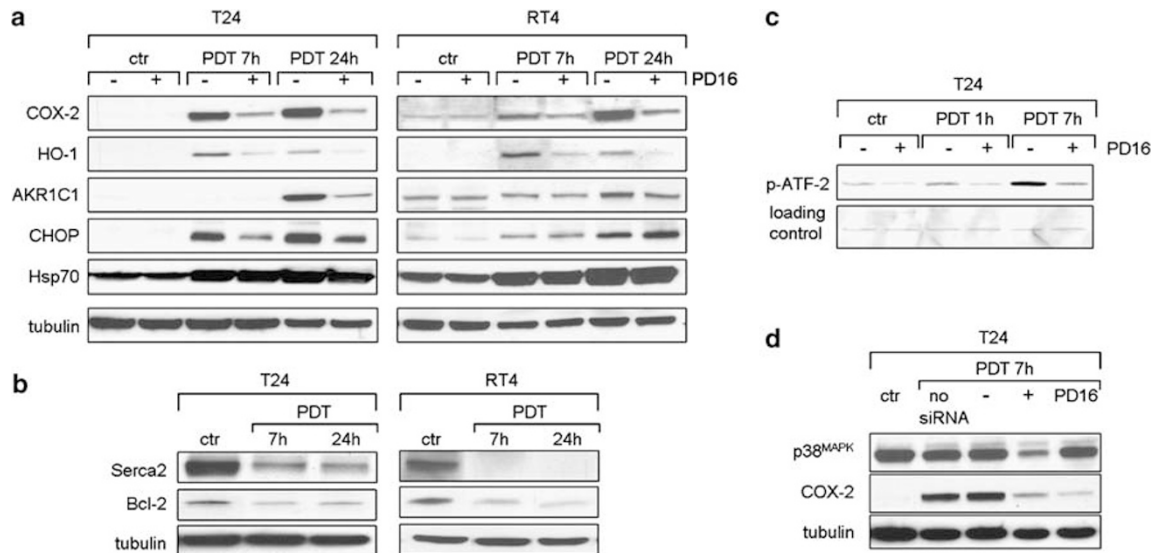


**Figure 3** Analysis of selected photodynamic therapy (PDT)-induced differentially expressed genes at the protein level. PDT-treated and control T24 and RT4 cells in the absence or presence of  $1 \mu\text{M}$  PD169316 were harvested at indicated time points after irradiation and subjected to western blot analysis using specific anti-COX-2, -HO-1, -AKR1C1, -CHOP and -Hsp70 antibodies (a), and anti-Serca2 and -Bcl-2 antibodies (b). (c) *In vitro* p38<sup>MAPK</sup> assay using the substrate GST-ATF-2 in control and PDT-treated T24 cells at indicated time points after irradiation. (d) T24 cells were transfected with siRNA ('-' represents 100 nM negative control siRNA Alexa Fluor 488, and '+' represents 100 nM siRNA SMARTpool p38<sup>MAPK</sup>) 72 h before PDT. PD169316 was added as control for p38<sup>MAPK</sup> inhibition. Control and PDT-treated cells were harvested 7 h after irradiation, and subjected to western blot analysis using specific anti-p38<sup>MAPK</sup> and -COX-2 antibodies. (a, b and d) Equal protein levels were confirmed with a specific anti-tubulin antibody.

bladder cancer cell lines with a different genetic background (Sanchez-Carbayo *et al.*, 2002).

Western blotting was performed to test whether microarray results accurately predicted changes in protein expression. Five highly induced genes (*PTGS2*, *HMOX1*, *AKR1C1*, *DDIT3*, *HSPA6*) covering key PDT-regulated biological processes were examined. Unfortunately, the poor specificity of commercially available matrix metalloproteinase (MMP) antibodies prevented accurate protein expression analysis of these PDT targets. *ATP2A2*, the sarco(endo)plasmic-reticulum  $\text{Ca}^{2+}$ -ATPase (SERCA) and *BCL2* were taken as paradigms of PDT down-regulated genes (Table 1).

Directional changes in protein expression were consistent with the differential PDT effect on corresponding transcripts as determined by microarray analysis of the T24 cells. COX-2 and AKR1C1 protein expression levels, but not Hsp70, were strongly repressed in the presence of PD169316 (Figure 3a, left panels), which clearly inhibited p38<sup>MAPK</sup> activity (Figure 3c). Moreover, specific effects of PD169316 were confirmed by p38<sup>MAPK</sup> siRNA knockdown, which dramatically affected the induction of COX-2, a key p38<sup>MAPK</sup> target (Figure 3d). PD169316-repressed heme oxygenase 1 (HO-1) and surprisingly also CHOP induction by PDT at the protein level (Figure 3a, left panels), to an extent unpredictable from qRT-PCR (Figure 2a) or evidenced by microarray analysis (Table 2).

The increase in protein levels of the main targets HO-1, COX-2, Hsp70, as well as the decline of SERCA2 and Bcl-2 proteins after hypericin-PDT in RT4 (Figures 3a and b, right panels) and in the invasive bladder cancer J82 cells (data not shown), were consistent with the

pattern observed in T24 cells. Also the data on the p38<sup>MAPK</sup> dependence were largely similar in all bladder cancer cells examined. A notable exception was CHOP whose induction after PDT in RT4 (Figure 3a, right panel) and J82 cells (data not shown) was not affected by PD169316, implying a cell line-specific regulation of this ER stress effector. The PDT-mediated induction of the AKR1C1 protein was reduced in the RT4 and J82 cells as compared to the T24 cells. However, slight but consistent p38<sup>MAPK</sup>-dependent stimulation in the AKR1C1 protein level in response to PDT could be still detected in the RT4 cells (Figure 3a, right panel).

#### *p38<sup>MAPK</sup> is required for growth and migratory capacity of the PDT-surviving cells*

Given the established role of several p38<sup>MAPK</sup>-dependent transcripts in carcinogenesis, we investigated the long-term biological relevance of p38<sup>MAPK</sup> inhibition on growth and migration of T24 cells surviving PDT. T24 cells were PDT treated in the presence or absence of PD169316 and 24 h after irradiation of the apoptotic cells, as revealed by active/processed caspase-3 (data not shown), were separated from the surviving cell fraction. The proliferation capacity of the surviving cells was monitored during several days, after replating them in 0.5% fetal calf serum (FCS) containing medium ('basal medium') or in their own medium (medium collected 24 h after PDT: 'conditioned medium'). Although the surviving cells cultured in basal medium were initially unable to proliferate, they dramatically regained their proliferation capacity in time (12 days) (Figures 4a and b, upper right panel), indicating an autocrine ability to

growth in low serum conditions. Surviving cells cultured in their own PDT-conditioned medium maintained their proliferation capacity throughout, indicating that this medium is enriched in factors required for their proliferation. Importantly, PD169316 completely abolished this growth competence (Figures 4a and b, upper right panel), strongly suggesting that the release of growth-promoting factors depends on the activation of the p38<sup>MAPK</sup> signaling cascades.

Subsequently, we evaluated the proliferation of control T24 cells cultured in 'basal medium' or in PDT-conditioned medium. Control cells readily proliferated reaching confluency after 12 days when cultured in conditioned medium (Figures 4a and b, upper left panel). This indicates that PDT-treated cells release factors able to stimulate in a paracrine way the proliferation of neighboring, nonaffected cells. Conversely, control cells ceased to proliferate when cultured in basal medium or in

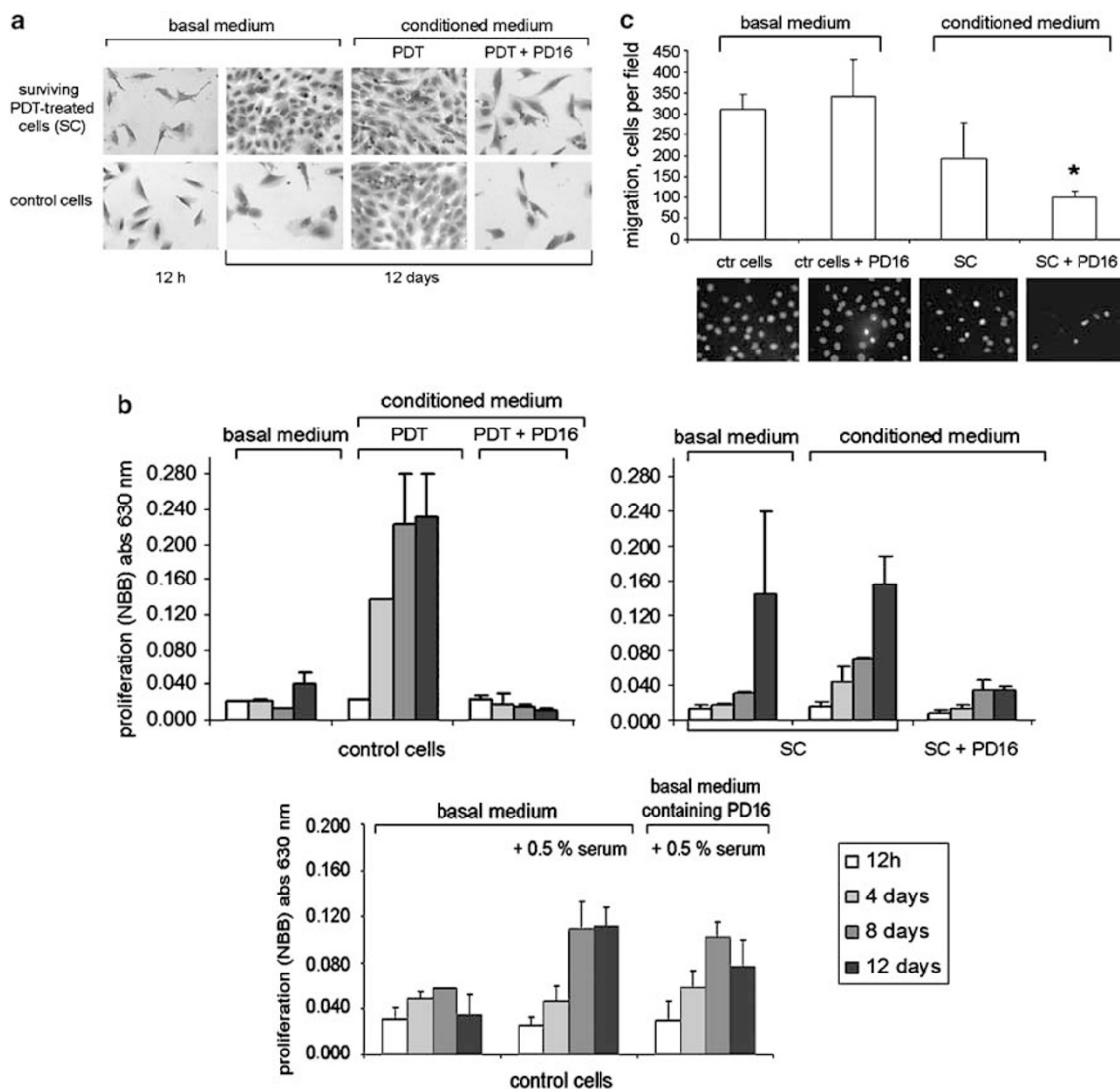


**Figure 4** p38MAPK plays a key role in growth and migration of T24 cells surviving photodynamic therapy (PDT)-treatment. T24 cells were PDT treated in 0.5% FCS DMEM. 1  $\mu$ M PD169316 was added 1 h prior to irradiation, where indicated. Cells used in the migration assay were kept in 0.5% FCS DMEM for 24 h prior to irradiation. (a) Proliferation of control and surviving PDT-treated T24 cells (SC) (24 h after irradiation), in the absence or presence of PD169316, was assayed as described in 'Materials and methods' section. Medium from control cells is indicated 'basal medium', whereas 'conditioned medium' is collected from PDT-treated cells, with or without PD169316 as indicated. Representative light microscopic pictures were taken from cells visualized with 0.1% crystal violet. (b) Upper panels: time-dependent proliferation of conditions described in (a) measured by naphthol blue black absorbance. A representative graph from three independent experiments is shown. Error bars represent s.d. of duplicated measurements. Lower panel: proliferation of control T24 cells in basal medium in the absence or presence of PD169316 after addition of 0.5% serum. (c) Migration of control and surviving PDT-treated T24 cells (SC), in the absence or presence of PD169316, resuspended and replated in basal or conditioned medium as indicated in 'Materials and methods' section. The inhibitors were readded to the medium before replating the cells. After 12 h, migrated cells were counted (at least five random fields were counted per condition). A representative graph is shown for at least three independent experiments. Error bars represent s.d. of at least five counted fields. Statistical analysis was performed by Student's *t*-test with  $P < 0.05$  (\*) as criteria of significance between 'SC' and 'SC + PD16' conditions. Details of representative fluorescent microscopic pictures are presented (lower panel).

conditioned medium derived from PDT-treated cells in the presence of PD169316. The addition of PD169316 to the basal medium did not significantly affect the proliferation capacity of control T24 cells, thus ruling out a direct effect of this inhibitor on cell growth (Figure 4b, lower panel).

Next, we evaluated the migratory potential of the surviving PDT-treated T24 cells and the impact of PD169316 on this tumor-promoting process (Figure 4c). A similar number of control or PDT-treated T24 cells, in the absence or presence of PD169316, were subjected to a transwell migration assay 24 h after PDT. Note that within the first day the growth rate of surviving PDT-treated and control cells did not vary significantly (Figure 4b, upper panels), thus measurable differences in migration cannot be explained by differences in the amount of cells at the time of the migration detection (12 h). Although at this postirradiation time point the PDT-treated cancer cells exhibited an attenuated pro-migratory ability as compared to control T24 cells, their migration was critically inhibited by PD169316 (Figure 4c).

## Discussion

Using oligonucleotide microarray analysis, we unraveled the coordinated expression of a gene cluster involved in cell death regulation after hypericin-PDT and additionally identified new p38<sup>MAPK</sup>-dependent targets and signaling pathways. This approach was not explored in previous studies with other photosensitizers (Verwanger *et al.*, 2002; Makowski *et al.*, 2003; Wild *et al.*, 2005) which utilized more restricted microarray platforms, thereby analysing the global PDT responses on a limited gene set.

Our analysis reveals a coordinated upregulation by PDT of several Hsp family members of molecular chaperones involved in cytoprotection (Calderwood *et al.*, 2006) and transcripts implicated in the UPR. PDT induced different molecular UPR components; induction of genes encoding ER-resident chaperones to assist correct protein folding (through XBP-1), translational attenuation to alleviate protein load on the ER (through the PERK-eIF2 $\alpha$ -ATF4 pathway) and ERAD to degrade ER-accumulated unfolded proteins (through HERPUD1) (Schroder and Kaufman, 2005). Since the most apical biochemical event in hypericin-photosensitized cells is the fast ER Ca<sup>2+</sup> depletion induced by SERCA photooxidation (Buytaert *et al.*, 2006), our data suggest that ER perturbations caused by the accumulation of photooxidized/misfolded proteins can persistently activate the UPR pathway.

Cell fate following ER stress and UPR induction is not fully understood, but increasing evidence indicates that this pathway is used to induce both adaptive and cell death responses and could affect tumor growth, promote dormancy and influence therapy outcome (Ma and Hendershot, 2004). Intriguingly, parallel to UPR induction hypericin-PDT induces Atgs (Table 1), suggesting that this cellular degradation process may be initiated to

reestablish ER homeostasis following photodamage. This is supported by recent studies pointing to ER stress as a powerful inducer of autophagy (Ogata *et al.*, 2006; Yorimitsu *et al.*, 2006). Recently we have shown that autophagy induced by hypericin-PDT in mouse embryonic fibroblasts under apoptosis-deficient conditions (for example, Bax/Bak double knockout) turns into a lethal pathway (Buytaert *et al.*, 2006), possibly due to increased persistence in the absence of caspase signaling. However, more studies are required to understand the role of autophagy and its relationship with the UPR in apoptosis-competent cells.

When ER stress is persistent and insoluble, sustained UPR leads to cell death, which can be mediated through CHOP-dependent targets (Marciniak *et al.*, 2004; Szegezdi *et al.*, 2006). PDT-mediated apoptosis with a mitochondrial- and ER-localizing porphyrin was shown to be attenuated in *chop*-deficient cells (Wong *et al.*, 2004). Thus, CHOP expression may contribute to efficient apoptosis induction by PDT initiated by ER photodamage and it is tempting to speculate that repression of Bcl-2 expression (Table 1 and Figure 3b) by hypericin-PDT in bladder cancer cells may result from CHOP activation and is mechanistically involved in photo killing.

This study further reveals key cellular PDT-responses critically influenced by the p38<sup>MAPK</sup> pathway. The pleiotropic p38<sup>MAPK</sup> appears to contribute to carcinogenesis by regulating growth factor expression (Elenitoba-Johnson *et al.*, 2003; Tsai *et al.*, 2003; Lin *et al.*, 2004), inflammatory- (Park *et al.*, 2003), and invasion-associated genes, including members of the MMP family (Johansson *et al.*, 2000; Reunanen *et al.*, 2002; Suarez-Cuervo *et al.*, 2004; Huang *et al.*, 2005).

Our results confirm the crucial role of p38<sup>MAPK</sup> in modulating immune and inflammatory responses by upregulation of for example, *COX-2*, *IL8* and *CSF2*, and additionally assign novel important molecular functions to this pathway in PDT signaling. Accordingly, we show the p38<sup>MAPK</sup>-coordinated induction by PDT of selected genes encoding 'phase 2 enzymes' including *AKRIC1*, *AKRIC3*, *GCLC*, *NQO1* (Table 2 and Figure 2) as well as *HMOX1* (Figures 2 and 3). These cytoprotective genes are induced by oxidants and electrophilic carcinogens through activation of the redox-dependent Keap1/Nrf2 pathway (Itoh *et al.*, 1999; Lee and Johnson, 2004). Accordingly, we recently observed that the activation of PI3K and p38<sup>MAPK</sup> signaling pathways by PDT contributes to HO-1 protein induction and survival through a mechanism involving nuclear accumulation of Nrf2 (Kocanova *et al.*, 2007). Thus p38<sup>MAPK</sup> may indeed attenuate oxidative stress following PDT through the regulation of the Nrf2/Keap1 system. Furthermore our study reveals that MMP-13, a member of the collagenase subfamily of MMPs, is a p38<sup>MAPK</sup> target. MMP-13 is expressed at the invading edges of urinary bladder transitional cell carcinoma (TCC) *in vivo*, and is regulated *in vitro* in T24 cells stimulated by tumor necrosis factor- $\alpha$  (TNF- $\alpha$ ) through p38<sup>MAPK</sup> (Bostrom *et al.*, 2000). *MMP-13* upregulation in bladder cancer cells after PDT is

remarkably p38<sup>MAPK</sup> dependent suggesting that p38<sup>MAPK</sup> inhibition could be required to halt the invasiveness of cancer cells escaping photokilling.

Interestingly, about 25% of the p38<sup>MAPK</sup>-dependent transcripts (for example, *IL8*, *MMP13*, *PTGS2*, *PLAGL2*, *CSF2*, *STK3*, *PTHLH*, *EREG*) contain in the 3' untranslated region adenylate/uridylylate-rich elements (AREs) ([http://rc.kfshrc.edu.sa/ARED/ARED\\_GENE/graphics/ARE.html](http://rc.kfshrc.edu.sa/ARED/ARED_GENE/graphics/ARE.html)), regulatory sequences in mRNA of genes involved in acute responses, including cytokines, growth factors and proto-oncogenes (Espel, 2005). Thus, the p38<sup>MAPK</sup> pathway in PDT-treated T24 cells could rapidly stabilize and increase translation of AREs-containing labile mRNAs, for example, for MMP-13, COX-2 and GM-CSF, involved in tumor promotion (Hashimoto *et al.*, 2000; Hoffmann *et al.*, 2002; Dean *et al.*, 2004).

The p38<sup>MAPK</sup>-dependent PDT-induced CHOP expression in T24 cells (Figure 3a, left panel) is intriguing, as it points to regulation of cell death modulators of the ER stress pathway. CHOP can be post-translationally activated by p38<sup>MAPK</sup> through phosphorylation at Ser78 and Ser81 (Wang and Ron, 1996) and a p38<sup>MAPK</sup> antagonist represses peroxynitrite-induced CHOP mRNA and protein expression (Oh-Hashi *et al.*, 2001). Since CHOP induction has been linked to cell death following prolonged ER stress, the p38<sup>MAPK</sup> pathway could paradoxically also induce the expression of cell death modulators after PDT. However, the p38<sup>MAPK</sup> inhibitor effect on CHOP protein expression appears to depend on the bladder cancer cell line examined (Figure 3b) and further studies linking p38<sup>MAPK</sup> activation to ER stress-induced CHOP activation and cell death are required.

This study unquestionably shows that supporting a cancer-prone phenotype is a major long-term biological function of the PDT-activated p38<sup>MAPK</sup> pathway. This notion is based on the evidence that p38<sup>MAPK</sup> not only drives regrowth and supports migration of 'undead' cells after PDT, but also enforces in a paracrine fashion the growth of nonaffected cancer cells.

Although PDT-induced p38<sup>MAPK</sup> orchestrates the induction of several genes involved in carcinogenesis, it is tempting to speculate that one of its major downstream effectors may be the release of soluble COX-2 metabolites (for example, prostaglandin (PG)E<sub>2</sub>). A recent study in human T cells shows that a PGE<sub>2</sub>-mediated stimulation of p38<sup>MAPK</sup> is involved in IL-8 transcription (Caristi *et al.*, 2005) through CHOP activation, raising the intriguing possibility that a PGE<sub>2</sub>-dependent positive feedback could maintain p38<sup>MAPK</sup> signaling and stimulate secondary responses dependent on this pathway. Thus, the role of p38<sup>MAPK</sup>-COX-2-PGE<sub>2</sub> cascade in the modulation of tumor growth as well as the immune response *in vivo* deserves to be further addressed.

## Materials and methods

### Materials

Hypericin was purified and stored as in Hendrickx *et al.*, 2003. Cell culture products were from Cambrex (Verviers, Belgium)

and FCS from Perbio Hyclone (Erembodegem, Belgium). Antibodies were purchased from Biomol Research Laboratories (Plymouth, PA, USA) (anti-caspase-3), Santa Cruz (Santa Cruz, CA, USA) (anti-COX-2, -Hsp70, -HO-1, -CHOP), Abnova (Taipei, Taiwan) (anti-AKR1C1), Pharmingen (San Diego, CA, USA) (anti-Bcl-2) and Sigma (Saint Louis, MO, USA) (anti- $\alpha$ -tubulin). The SERCA2b antibody was kindly provided by Dr F Wuytack (KULeuven, Belgium). Secondary antibodies were from DAKO (Glostrup, Denmark). PD169316 was from Calbiochem (San Diego, CA, USA).

### Cell culture, photosensitization and siRNA transfection

T24 and RT4 cells (human TCC of the bladder) were preincubated with 150 nM hypericin for 16 h in subdued light conditions (<1  $\mu$ W cm<sup>-2</sup>) followed by irradiation (4 J cm<sup>-2</sup>) in Dulbecco's modified Eagle's medium (DMEM) ('PDT-treated') as described (Hendrickx *et al.*, 2003). 'Controls' are cells preincubated with 150 nM hypericin, but not subsequently irradiated. Total cell lysates were prepared (Buytaert *et al.*, 2006) at indicated time points following irradiation. p38<sup>MAPK</sup> activity was measured using a p38<sup>MAPK</sup> kinase assay kit from Cell Signaling (Beverly, MA, USA), according to the manufacturer's instructions. Transfection of T24 cells with 100 nM siRNA SMARTpool p38<sup>MAPK</sup> (Upstate/Dharmacon, Waltham, MA, USA) or Negative Control siRNA Alexa Fluor 488 (Qiagen, Venlo, Netherlands) was performed as described (Kocanova *et al.*, 2007).

### Affymetrix microarrays

Total RNA was isolated using the RNeasy Mini kit (Qiagen) from two independent experiments performed in duplicate generating four hybridizations per sample. RNA quality and concentration was determined using Agilent 2100 bioanalyzer (Agilent Technologies, Palo Alto, CA, USA). Samples were prepared for microarray hybridization on Affymetrix GeneChip HG-U133A 2.0 arrays, according to the manufacturer's instructions (Affymetrix, Santa Clara, CA, USA).

### Analysis of microarrays

Microarray data preprocessing and analysis was performed using Bioconductor software (Gentleman *et al.*, 2004) implemented in the statistical programming environment R. The data, containing four samples (control T24 cells and PDT-treated T24 cells at 7 h after irradiation, each in the presence and absence of PD169316) and four repeats of each sample, were normalized using the GC Robust Multi-array Average (GCRMA) method (Wu *et al.*, 2004). MAS5.0 present/absent calls were calculated and features with over 13 out of 16 absent calls were regarded as not expressed in the whole experiment and removed from further analysis. After filtering, 14488 features remained. Subsequently differential expression was determined using the linear models method implemented in the limma package. Obtained *P*-values were adjusted for multiple testing using the false discovery rate-based *P*-value adjustment (Benjamini and Hochberg, 1995). Threshold for differential expression was <0.05 on the adjusted *P*-values. Comparison of the gene expression profiles in control cells with or without PD169316 indicated that the inhibitor by itself had a negligible impact as it resulted in the differential expression of only one gene (*SERPINA1* fold change: 1.96, *P*=0.008). Selected differential expressed genes were annotated with GO identifiers using the biomaRt package (Durinck *et al.*, 2005), which retrieves data from Ensembl (Birney *et al.*, 2006). These GO terms were mapped to the generic GO slim available from the GO website (<http://www.geneontology.org>). Actual mapping

was performed using the map2slim Perl script, also available from the GO website.

#### Real-time quantitative PCR

cDNA was prepared in a 20 µl final volume with 1 µg RNA as described (Volanti *et al.*, 2004). cDNA (2 µl) was mixed with 10 µl SYBR Green Mix (Applied Biosystems, Warrington, UK) and forward and reverse primers for each gene of interest, or with 300 nM forward (5'-GAGTATGCCTGCCGTGTG-3') and 300 nM reverse (5'-AATCCAAATGCGGCATCT-3') β2-microglobulin (B2M) primers in a 20 µl final volume. Real-time PCR was performed with the ABI-PRISM 7000 Sequence Detection System (Applied Biosystems). Data were subjected to relative quantification using the comparative  $C_T$  ( $\Delta\Delta C_T$ ) method, where B2M was used as an endogenous reference for normalization. The following arithmetic formula was applied to each sample, and the results plotted in fold induction:

$$2^{-(C_T^{\text{treated}} - C_T^{\text{untreated}})_{\text{gene}} - (C_T^{\text{treated}} - C_T^{\text{untreated}})_{\text{B2M}}}$$

Primers sequence and concentration: MMP1F (270 nM): 5'-CC TCGCTGGGAGCAAACA-3'; MMP1R (270 nM): 5'-TTGGC AAATCTGGCGTGTAAAT-3'; MMP10F (540 nM): 5'-TTGGC CCTCTCTTCCATCAT-3'; MMP10R (540 nM): 5'-AAACGG TGTCCCTGCTGTAA-3'; MMP13F (810 nM): 5'-TGTTGCT GCGCATGAGTTC-3'; MMP13R (810 nM): 5'-TGCTCCA GGGTCCTTGGA-3'; AKR1C1F (540 nM): 5'-GATCCCACC GAGAAGAACA-3'; AKR1C1R (540 nM): 5'-AAAGGAC TGGTCTCCAAGA-3'; HO-1F (270 nM): 5'-CTGAGTTCA TGAGAACTTTCAGAAG-3'; HO-1R (270 nM): 5'-TGGTA CAGGGAGGCCATCAC-3'.

#### Proliferation and migration assays

Prior to irradiation, T24 cells were washed with phosphate-buffered saline and replaced in DMEM containing 0.5% FCS, with or without PD169316 as detailed in figure legends. After 24 h of irradiation, control and surviving PDT-treated cells were collected, resuspended in basal or different conditioned media as indicated and replated either in collagen I-coated 96-well plates ( $0.005 \times 10^6$  cells per well) or in the upper chamber of transwells ( $20 \times 10^3$  cells) for proliferation or migration assays, respectively.

**Proliferation assay** Proliferation assay at indicated time points after replating and cell proliferation was measured by

naphthol blue black (NBB) (Acros Organics, Geel, Belgium) assay. Briefly, cells were fixed in 10% formaldehyde for 10 min, washed and incubated with 0.05% NBB for 30 min at 37 °C. After washing, NBB was eluted with 50 mM NaOH for 1 h at room temperature, and absorbance was measured at 630 nm.

**Migration assay** Migration of control or surviving PDT-treated T24 cells was analysed through polycarbonate filters (8 µm pore size) (Elscolab, Kruibeke, Belgium) coated with type I collagen (BD Biosciences, Bedford, MA, USA) (modified Boyden chamber). Medium (10% FCS) was placed in the lower chamber as chemoattractant. Following a 12 h incubation period, nonmigrated cells on the upper surface of the filter were removed, and the cells migrated through the filter were fixed, washed and counted manually by fluorescence microscopy after visualizing cell nuclei with 4',6-diamidino-2-phenylindol -containing Vectashield mounting medium (Vector, Burlingame, CA, USA).

#### Abbreviations

AREs, adenylate/uridylylate-rich elements; ATF, activating transcription factor; Atg, autophagy-related gene; CHOP, C/EBP homologous protein; COX-2, cyclooxygenase-2; ECM, extracellular matrix; ER, endoplasmic reticulum; ERAD, ER-associated degradation; GO, Gene Ontology; GM-CSF, granulocyte macrophage colony-stimulating factor; HO-1, heme oxygenase 1; Hsp, heat shock protein; MAPK, mitogen-activated protein kinase; MMP, matrix metalloproteinase; Nrf2, NF-E2-related factor 2; PDT, photodynamic therapy; PG, prostaglandin; PERK, pancreatic ER kinase (PKR)-like ER kinase; ROS, reactive oxygen species; SERCA, sarco(endo)plasmic-reticulum  $\text{Ca}^{2+}$ -ATPase; TCC, transitional cell carcinoma; UPR, unfolded protein response.

#### Acknowledgements

We thank Dr B Hennuy (Head of Transcriptomics—GIGA University of Liège, Belgium) for excellent handling of the microarray experiments. This work was supported by the Geconcerteerde Onderzoeksacties (GOA) and Onderzoekstoelag (OT) from the KULeuven, the Interuniversitaire Attractiepolen (IAP, Vi/P18) of the Federal Belgian Government and by FWO grant G.0104.02.

#### References

- Agostinis P, Buytaert E, Breysens H, Hendrickx N. (2004). Regulatory pathways in photodynamic therapy induced apoptosis. *Photochem Photobiol Sci* **3**: 721–729.
- Assefa Z, Vantieghem A, Declercq W, Vandenebeele P, Vandenebeede JR, Merlevede W *et al.* (1999). The activation of the c-Jun N-terminal kinase and p38 mitogen-activated protein kinase signaling pathways protects HeLa cells from apoptosis following photodynamic therapy with hypericin. *J Biol Chem* **274**: 8788–8796.
- Benjamini Y, Hochberg Y. (1995). Controlling the false discovery rate: a practical and powerful approach to multiple testing. *J R Stat Soc, B* **57**: 289–300.
- Birney E, Andrews D, Caccamo M, Chen Y, Clarke L, Coates G *et al.* (2006). Ensembl 2006. *Nucleic Acids Res* **34**: D556–D561.
- Bostrom PJ, Ravanti L, Reunanen N, Aaltonen V, Soderstrom KO, Kahari VM *et al.* (2000). Expression of collagenase-3 (matrix metalloproteinase-13) in transitional-cell carcinoma of the urinary bladder. *Int J Cancer* **88**: 417–423.
- Buytaert E, Callewaert G, Hendrickx N, Scorrano L, Hartmann D, Missiaen L *et al.* (2006). Role of endoplasmic reticulum depletion and multidomain proapoptotic BAX and BAK proteins in shaping cell death after hypericin-mediated photodynamic therapy. *FASEB J* **20**: 756–758.
- Calderwood SK, Khaleque MA, Sawyer DB, Ciocca DR. (2006). Heat shock proteins in cancer: chaperones of tumorigenesis. *Trends Biochem Sci* **31**: 164–172.
- Caristi S, Piraino G, Cucinotta M, Valenti A, Loddo S, Teti D. (2005). Prostaglandin E2 induces interleukin-8 gene transcription by activating C/EBP homologous protein in human T lymphocytes. *J Biol Chem* **280**: 14433–14442.
- Castano AP, Mroz P, Hamblin MR. (2006). Photodynamic therapy and anti-tumour immunity. *Nat Rev Cancer* **6**: 535–545.
- Dean JR, Sully G, Clark AR, Saklatvala J. (2004). The involvement of AU-rich element-binding proteins in p38 mitogen-activated protein kinase pathway-mediated mRNA stabilisation. *Cell Signal* **16**: 1113–1121.

- D'Hallewin MA, Kamuhabwa AR, Roskams T, de Witte PA, Baert L. (2002). Hypericin-based fluorescence diagnosis of bladder carcinoma. *BJU Int* **89**: 760–763.
- Dolmans DE, Fukumura D, Jain RK. (2003). Photodynamic therapy for cancer. *Nat Rev Cancer* **3**: 380–387.
- Durinck S, Moreau Y, Kasprzyk A, Davis S, De Moor B, Brazma A *et al.* (2005). BioMart and bioconductor: a powerful link between biological databases and microarray data analysis. *Bioinformatics* **21**: 3439–3440.
- Elenitoba-Johnson KS, Jenson SD, Abbott RT, Palais RA, Bohling SD, Lin Z *et al.* (2003). Involvement of multiple signaling pathways in follicular lymphoma transformation: p38-mitogen-activated protein kinase as a target for therapy. *Proc Natl Acad Sci USA* **100**: 7259–7264.
- Espel E. (2005). The role of the AU-rich elements of mRNAs in controlling translation. *Semin Cell Dev Biol* **16**: 59–67.
- Gentleman RC, Carey VJ, Bates DM, Bolstad B, Dettling M, Dudoit S *et al.* (2004). Bioconductor: open software development for computational biology and bioinformatics. *Genome Biol* **5**: R80.
- Hashimoto S, Matsumoto K, Gon Y, Maruoka S, Kujime K, Hayashi S *et al.* (2000). p38 MAP kinase regulates TNF alpha-, IL-1 alpha- and PAF-induced RANTES and GM-CSF production by human bronchial epithelial cells. *Clin Exp Allergy* **30**: 48–55.
- Hendrickx N, Volanti C, Moens U, Seternes OM, de Witte P, Vandenheede JR *et al.* (2003). Up-regulation of cyclooxygenase-2 and apoptosis resistance by p38 MAPK in hypericin-mediated photodynamic therapy of human cancer cells. *J Biol Chem* **278**: 52231–52239.
- Hoffmann E, Dittrich-Breiholz O, Holtmann H, Kracht M. (2002). Multiple control of interleukin-8 gene expression. *J Leukoc Biol* **72**: 847–855.
- Hori O, Miyazaki M, Tamatani T, Ozawa K, Takano K, Okabe M *et al.* (2006). Deletion of SERP1/RAMP4, a component of the endoplasmic reticulum (ER) translocation sites, leads to ER stress. *Mol Cell Biol* **26**: 4257–4267.
- Huang X, Chen S, Xu L, Liu Y, Deb DK, Platanius LC *et al.* (2005). Genistein inhibits p38 map kinase activation, matrix metalloproteinase type 2, and cell invasion in human prostate epithelial cells. *Cancer Res* **65**: 3470–3478.
- Imasato A, Desbois-Mouthon C, Han J, Kai H, Cato AC, Akira S *et al.* (2002). Inhibition of p38 MAPK by glucocorticoids via induction of MAPK phosphatase-1 enhances nontypable Haemophilus influenzae-induced expression of toll-like receptor 2. *J Biol Chem* **277**: 47444–47450.
- Itoh K, Ishii T, Wakabayashi N, Yamamoto M. (1999). Regulatory mechanisms of cellular response to oxidative stress. *Free Radic Res* **31**: 319–324.
- Jiang HY, Wek SA, McGrath BC, Lu D, Hai T, Harding HP *et al.* (2004). Activating transcription factor 3 is integral to the eukaryotic initiation factor 2 kinase stress response. *Mol Cell Biol* **24**: 1365–1377.
- Johansson N, la-aho R, Uitto V, Grenman R, Fusenig NE, Lopez-Otin C *et al.* (2000). Expression of collagenase-3 (MMP-13) and collagenase-1 (MMP-1) by transformed keratinocytes is dependent on the activity of p38 mitogen-activated protein kinase. *J Cell Sci* **113**: 227–235.
- Kamuhabwa A, Agostinis P, Ahmed B, Landuyt W, Van Cleynenbreugel B, Van Poppel H *et al.* (2004). Hypericin as a potential phototherapeutic agent in superficial transitional cell carcinoma of the bladder. *Photochem Photobiol Sci* **3**: 772–780.
- Kocanova S, Buytaert E, Matroule JY, Piette J, Golab J, de Witte P *et al.* (2007). Induction of heme-oxygenase 1 requires the p38(MAPK) and PI3K pathways and suppresses apoptotic cell death following hypericin-mediated photodynamic therapy. *Apoptosis* **12**: 731–741.
- Lee JM, Calkins MJ, Chan K, Kan YW, Johnson JA. (2003). Identification of the NF-E2-related factor-2-dependent genes conferring protection against oxidative stress in primary cortical astrocytes using oligonucleotide microarray analysis. *J Biol Chem* **278**: 12029–12038.
- Lee JM, Johnson JA. (2004). An important role of Nrf2-ARE pathway in the cellular defense mechanism. *J Biochem Mol Biol* **37**: 139–143.
- Lin Z, Crockett DK, Jenson SD, Lim MS, Elenitoba-Johnson KS. (2004). Quantitative proteomic and transcriptional analysis of the response to the p38 mitogen-activated protein kinase inhibitor SB203580 in transformed follicular lymphoma cells. *Mol Cell Proteomics* **3**: 820–833.
- Liu RY, Fan C, Liu G, Olashaw NE, Zuckerman KS. (2000). Activation of p38 mitogen-activated protein kinase is required for tumor necrosis factor-alpha-supported proliferation of leukemia and lymphoma cell lines. *J Biol Chem* **275**: 21086–21093.
- Lou H, Du S, Ji Q, Stolz A. (2006). Induction of AKR1C2 by phase II inducers: identification of a distal consensus antioxidant response element regulated by NRF2. *Mol Pharmacol* **69**: 1662–1672.
- Ma Y, Hendershot LM. (2004). Herp is dually regulated by both the endoplasmic reticulum stress-specific branch of the unfolded protein response and a branch that is shared with other cellular stress pathways. *J Biol Chem* **279**: 13792–13799.
- Makowski M, Grzela T, Niderla J, Lazarczyk M, Mroz P, Kopee M *et al.* (2003). Inhibition of cyclooxygenase-2 indirectly potentiates antitumor effects of photodynamic therapy in mice. *Clin Cancer Res* **9**: 5417–5422.
- Marciniak SJ, Yun CY, Ouyadomari S, Novoa I, Zhang Y, Jungreis R *et al.* (2004). CHOP induces death by promoting protein synthesis and oxidation in the stressed endoplasmic reticulum. *Genes Dev* **18**: 3066–3077.
- Ogata M, Hino SI, Saito A, Morikawa K, Kondo S, Kanemoto S *et al.* (2006). Autophagy is activated for cell survival after ER stress. *Mol Cell Biol* **26**: 9220–9231.
- Oh-Hashi K, Maruyama W, Isobe K. (2001). Peroxynitrite induces GADD34, 45, and 153 VIA p38 MAPK in human neuroblastoma SH-SY5Y cells. *Free Radic Biol Med* **30**: 213–221.
- Ohoka N, Yoshii S, Hattori T, Onozaki K, Hayashi H. (2005). TRB3, a novel ER stress-inducible gene, is induced via ATF4-CHOP pathway and is involved in cell death. *EMBO J* **24**: 1243–1255.
- Park JI, Lee MG, Cho K, Park BJ, Chae KS, Byun DS *et al.* (2003). Transforming growth factor-beta1 activates interleukin-6 expression in prostate cancer cells through the synergistic collaboration of the Smad2, p38-NF-kappaB, JNK, and Ras signaling pathways. *Oncogene* **22**: 4314–4332.
- Reunanen N, Li SP, Ahonen M, Foschi M, Han J, Kahari VM. (2002). Activation of p38 alpha MAPK enhances collagenase-1 (matrix metalloproteinase (MMP)-1) and stromelysin-1 (MMP-3) expression by mRNA stabilization. *J Biol Chem* **277**: 32360–32368.
- Sanchez-Carbayo M, Socci ND, Charytonowicz E, Lu M, Prystowsky M, Childs G *et al.* (2002). Molecular profiling of bladder cancer using cDNA microarrays: defining histogenesis and biological phenotypes. *Cancer Res* **62**: 6973–6980.
- Schroder M, Kaufman RJ. (2005). ER stress and the unfolded protein response. *Mutat Res* **569**: 29–63.
- Sengupta N, Siddiqui E, Mumtaz FH. (2004). Cancers of the bladder. *J R Soc Health* **124**: 228–229.
- Suarez-Cuervo C, Merrell MA, Watson L, Harris KW, Rosenthal EL, Vaananen HK *et al.* (2004). Breast cancer cells with inhibition of p38alpha have decreased MMP-9 activity and exhibit decreased bone metastasis in mice. *Clin Exp Metastasis* **21**: 525–533.
- Szegezdi E, Logue SE, Gorman AM, Samali A. (2006). Mediators of endoplasmic reticulum stress-induced apoptosis. *EMBO Rep* **7**: 880–885.
- Tsai PW, Shiah SG, Lin MT, Wu CW, Kuo ML. (2003). Up-regulation of vascular endothelial growth factor C in breast cancer cells by heregulin-beta 1. A critical role of p38/nuclear factor-kappa B signaling pathway. *J Biol Chem* **278**: 5750–5759.
- Van De Putte M, Roskams T, Vandenheede JR, Agostinis P, de Witte PA. (2005). Elucidation of the tumorigenic principle of hypericin. *Br J Cancer* **92**: 1406–1413.
- Verwanger T, Sanovic R, Aberger F, Frischauf AM, Krammer B. (2002). Gene expression pattern following photodynamic treatment of the carcinoma cell line A-431 analysed by cDNA arrays. *Int J Oncol* **21**: 1353–1359.

- Volanti C, Gloire G, Vanderplasschen A, Jacobs N, Habraken Y, Piette J. (2004). Downregulation of ICAM-1 and VCAM-1 expression in endothelial cells treated by photodynamic therapy. *Oncogene* **23**: 8649–8658.
- Wang XZ, Ron D. (1996). Stress-induced phosphorylation and activation of the transcription factor CHOP (GADD153) by p38 MAP Kinase. *Science* **272**: 1347–1349.
- Wild PJ, Krieg RC, Seidl J, Stoehr R, Reher K, Hofmann C *et al*. (2005). RNA expression profiling of normal and tumor cells following photodynamic therapy with 5-aminolevulinic acid-induced protoporphyrin IX *in vitro*. *Mol Cancer Ther* **4**: 516–528.
- Wong S, Luna M, Ferrario A, Gomer CJ. (2004). CHOP activation by photodynamic therapy increases treatment induced photosensitization. *Lasers Surg Med* **35**: 336–341.
- Wu Z, Irizarry R, Gentleman R, Murillo FM, Spencer F. (2004). A Model Based Background Adjustment for Oligonucleotide Expression Arrays. *J Am Stat Assoc* **99**: 909–917.
- Yorimitsu T, Nair U, Yang Z, Klionsky DJ. (2006). Endoplasmic reticulum stress triggers autophagy. *J Biol Chem* **281**: 30299–30304.
- Zarubin T, Han J. (2005). Activation and signaling of the p38 MAP kinase pathway. *Cell Res* **15**: 11–18.

Supplementary Information accompanies the paper on the Oncogene website (<http://www.nature.com/onc>).